



---

## **Design of Non-Isolated Dual Input Single Output Dc-Dc Converter for Electric Vehicles**

***Vavilapalli Tarun<sup>1</sup>, Kakula Vinay<sup>2</sup>, Sappati Sri Harsha<sup>3</sup>, S Jagadessh<sup>4</sup>, S Chathurya<sup>5</sup>***

*<sup>1,5</sup>B.Tech Student, Department of Electrical and Electronics Engineering, GMR Institute of Technology, Vizianagaram District, A.P, India*

---

### **ABSTRACT**

One of the important concerns in today's world is Environment pollution, at present world is trying to adapt different technologies for the protection of environment. Electric Vehicle Technology ensures saving the environment by replacing the conventional vehicles which are core reason for the air pollution. There are many challenging aspects in designing of the electric vehicles. One such aspect is energy management by designing the power electronic converters with less size and better efficiency. Based on the State of Charge of the electric vehicles, the energy can be transferred from the grid to the battery and battery to grid. For this purpose, we can design a Dual Input Single Output Converter (DISOC). Multi Input Single Output converters can be classified into Isolated and Non-Isolated. Isolated converters use high frequency transformer and more semi-conductors for interfacing the multiple inputs, which in turn increases the cost and size. Non isolated converters overcome those limitations. Based upon the State of Charge (SoC) of the vehicle, irradiance of solar photo voltaic cell and status of the Electric Vehicle.

---

Keywords:electric vehicle (EV), photo voltaic hybrid electric vehicle (PVHEV), hybrid electric vehicle (HEV), hybrid energy storage system (HESS), plug-in hybrid electric vehicle (PHEV), ultracapacitor (UC).

---

### **1. Main text**

The main focus in present world is to develop various technologies for the clean energy to protect environment. Solar energy, wind energy, fuel cells these are the various sources which are better replacement for the fossil fuels. Utilizing only one source for the propulsion of the vehicles may not be feasible and satisfy the load condition. Hybrid Energy Storage System is the one of the best approaches for fulfilling the load demand. In Hybrid Energy Storage System power electronic converter plays key role[1] – [9] . In traditional HES technologies parallelly connected single input converters are using, which bears more, number of components count and cost. Multi Input Multi Output converters can be the better alternative. Multi Input Converters are again classified into two types: Isolated Converters [10],[11], [12]and Non-isolated Converters. Deployment of Isolated converters uses high-frequency transformer and more, number of switches which increases complexity and cost of the converters. Non-isolated converters which have the direct electrical path between the load and source reduces the number of components and size of the converter.

## 2. Working and operation

### DISOC TOPOLOGY:

The designed DISOC circuit for EV application is illustrated in the following figure [13]. The circuit consists of one diode ( $D_1$ ), an inductor ( $L$ ), an output capacitor ( $C$ ), four relays, and three IGBTs with antiparallel diodes ( $S_2$ ,  $S_m$ , and  $S_{Bi}$ ) ( $R_1$ ,  $R_2$ ,  $R_3$  and  $R_A$ ). If not, when the switch  $S_2$  is turned on, the source  $V_1$  will be passed through by the relay  $R_A$ .

Main objective of this paper is to develop a novel DC-DC converter called DISOC that can incorporate multiple input energy sources. The following are the primary features of the DISOC are:

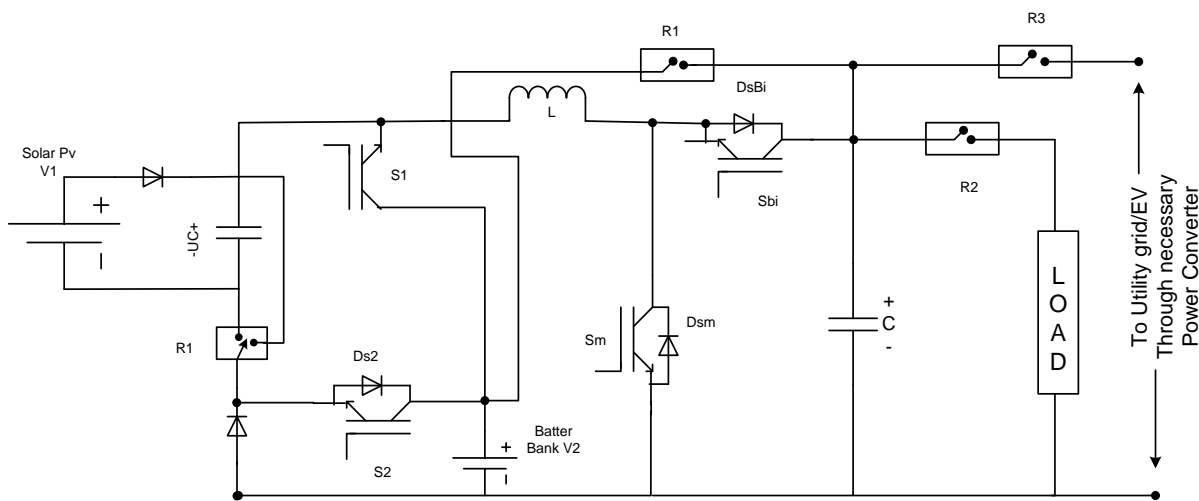


**Fig 2.1 The converter topology of DISOC in solar-powered vehicle**

i) We suggest employing two semiconductor switches, a diode, and two relays for the front-end converter structure. Even when one or more of the input sources is unavailable, the proposed converter is enabled by the structure. Equation 8 states that the switch  $S_2$  increases the output voltage by enabling the input sources to operate in cascade. ii) Relays are organized in DISOC in a particular manner that is compatible with the power converter structure. That arrangement enables DISOC to operate in six various modes. iii) The switch provides the DISOC the ability to operate the input sources in a cascaded approach and boosts output voltage. iv) The relay  $R_3$  enables the DISOC to perform the V2G and V2V. v) The relay  $R_1$  enables the DISOC to charge  $V_2$  from  $V_1$ . vi) The arrangement of the diode and the configuration of the input source  $V_1$  prevents the input from floating. vii) The suggested DISOC employs fewer parts and can operate in six different configurations while still utilizing the same converter configuration. viii) According to the loss breakdown analysis and efficiency profile, the suggested non-isolated dual-input single output DC-DC converter has reduced power losses and higher efficiency whenever compared to a few traditional converters.

The six different sorts of operations are carried out by the DISOC through proper control of the IGBTs. The level of charge (SOC) of the battery, the amount of solar PV radiation, and the status of the EV are used to determine the kind of operation. The converter can carry out the following six different types of operation with just one inductor.

Type i. Combinational boost operation (C-boost)

Type ii. Solar PV-powered operation

Type iii. Battery-powered operation

Type iv. Battery charging from solar PV in parking mode

Type v. Power flow from V2V or V2G in parking mode

Type vi. Bidirectional rear-buck operation

When a vehicle has a battery and photovoltaic cells as input sources, the combination boost type (Type I) operates by delivering power concurrently from

both sources to enhance the vehicle's speed. To drive the vehicle at a normal speed, the next two types of operations—solar PV-powered (Type ii) and battery-powered (Type iii) operations are used. Battery-powered operation is recommended when solar PV cannot supply the necessary power. The designed DISOC functions as a single input single-output (SISO) boost convert during Type ii and Type iii operations. Based on the battery's SOC, the following two types of operations (Type iv and Type v) are performed whenever the vehicle is in parking mode during the day. When the battery's SOC is less than full, Type iv utilizes the energy produced by solar PV to charge the battery. In this instance, the DISOC serves as a SISO boost converter.

The DISOC operates in three-way during Type V operation depending on the availability of solar PV and batteries. i) Solar energy alone is practical: Through a suitable inverter system, the DISOC behaves as a SISO boost converter and feeds solar PV power into the utility grid (V2G). When the converter is in V2G mode, a single-phase inverter system is used to send power into the utility grid. The DISOC feeds solar PV power into another EV during V2V operation. ii) Battery alone available: In this case, the DISOC functions as a SISO boost converter and pushes the battery's energy into the utility grid or another EV. In this case, the DISOC functions as a dual-input single-output (DISO) converter and transfers the electricity from the battery to the utility grid or the other EV. iii) Solar PV and battery both are available. As a result, the electricity generated by solar PV may be successfully used when parked, and the EV battery can be used to take part in the grid assistance programme. So that by contributing their energy sources under the V2G or V2V programme, the EV can generate excess revenue. where they use two or three conducting switches in each mode of operation.

### 3. Operation of DISOC topology:

The input sources of solar PV and battery are expressed as general voltage sources with voltages  $V_1$  and  $V_2$ , respectively, to describe how the converter operates. The motor driving system is substituted with a resistive load. For the examination of the DISOC, two input sources, such as  $V_1$  and  $V_2$ , are taken into consideration with the provision that  $V_2 > V_1$ . The DISOC can operate the relays  $R_1$ ,  $R_2$ ,  $R_3$ , and  $R_A$  to carry out six distinct types of operations. At continuous conduction mode (CCM), it has four modes of operation during Type i operation, whereas, the other Type of operations have only two modes.

#### 3.1 C-boost operation in CCM:

One of the aspects of the designed converter is the C-boost. The other relays are still in the off state, but the relays  $R_2$  and  $R_A$  are currently in the on condition. Depending on the input source, the C-boost operation can be carried out in three different ways, the fourth of which requires the inductor  $L$  operating in freewheeling mode. The waveforms below represent the output voltage waveforms of the inductor  $L$  of the following scenarios. i) When only the  $V_1$  freewheels ii) when  $V_1+V_2$  freewheels only the iii) when  $V_2$  freewheels. The output voltage delivered by the DISOC during C-boost is undisturbed by the fact that the charging order of the three input sources varies in the first three modes of operation. However, the output voltage is determined by the source's contribution in the fourth mode. In the CCM, the DISOC analysis for C-boost is completed. The following section explains the four C-boost operating modes when  $V_1$  freewheels in fourth mode.

##### Mode 1:

The above figure displays the mode-1 circuit schematic. The switches  $S_1$  and  $S_m$  are conducting in this mode, while the other switches are in the non-conducting condition. For the duty ratio of  $d_1$ , the inductor stores energy from the voltage source  $V_2$ , and the load is powered by the capacitor. Equation includes the value of the inductor current. Here,  $V_L=V$ .

Inductor current when  $V_2$  alone free wheels is:  $I_L = I_{L0} + \frac{1}{L}V_2d_1T$

##### Mode 2:

Diagram demonstrates how the DISOC operates in mode 2. The switches  $S_2$  and  $S_m$  are conduction during this mode, while the remaining switches are in the off state. The input sources  $V_1$  and  $V_2$  are connected in series when the switch  $S_2$  is turned on. As a result, for the duty ratio of  $d_2$ , the inductor continues to store the energy from both input sources at a voltage value of  $V_1+V_2$ . This is shown in Figure. The load continues to get power from the capacitor. This mode of operation's distinguishing feature is the simultaneous power transfer from two input sources to the load utilising only two semiconductor switches, as contrast to many switches used in traditional converters.

Inductor current when  $V_1 + V_2$  free wheels:  $I_L = I_{L1} + \frac{1}{L}(V_1 + V_2)d_2T$

##### Mode 3:

The above figure 4.2 illustrates the mode 3 circuit representation. In this case, only the switch  $S_m$  is turned on; all other switches are off. For the duration of the duty ratio  $d_3$ , the inductor keeps storing energy from  $V_1$ , and the capacitor keeps supplying the power to the load. The current in the inductor can be expressed as

$I_L = I_{L2} + \frac{1}{L}V_1(d_3 - d_2 - d_1)T$

##### Mode 4:

The equivalent circuit of the DISOC, which occurs when the inductor freewheels the stored energy into the load side through the source  $V_1$  and the diodes

$D_1$  and  $D_{S_{Bi}}$ , is seen in the figure 4.2 The switch  $S_m$  is off in this instance. The other switches,  $S_1$  and  $S_2$ , are still turned off. The voltage across the inductor terminals  $V_1 - V_0$ . Current in the inductor can be expressed as  $I_L = I_{Lp} + \frac{1}{L}(V_1 - V_0)(1 - d_3)T$

According to the volt-second balance principle, in a steady-state condition, the average voltage across the inductor is zero and it is expressed in equation  $V_2 d_1 + (V_1 + V_2) d_2 + V_1 (d_3 - (d_1 + d_2)) + (V_1 - V_0)(1 - d_3) = 0$

Whenever  $V_1 + V_2$  freewheel in the fourth mode, the DISOC's four operational modes in C-boost are used to calculate the output voltage's final expression, which is as follows.  $V_0 = \frac{V_1(1-d_1)+V_2(d_1+d_2)}{1-D}$

The final expression of the output voltage is derived using the four operational modes of the DISOC in C-boost when  $V_1 + V_2$  freewheels in the fourth mode as  $V_0 = \frac{V_1(1-d_2)+V_2(d_1+d_2)}{1-D}$

Similar to this, when  $V_2$  freewheels in fourth mode, the final expression of the output voltage of the DISOC is estimated as  $V_0 = \frac{V_1(d_1+d_2)+V_2(1-d_1)}{1-D}$

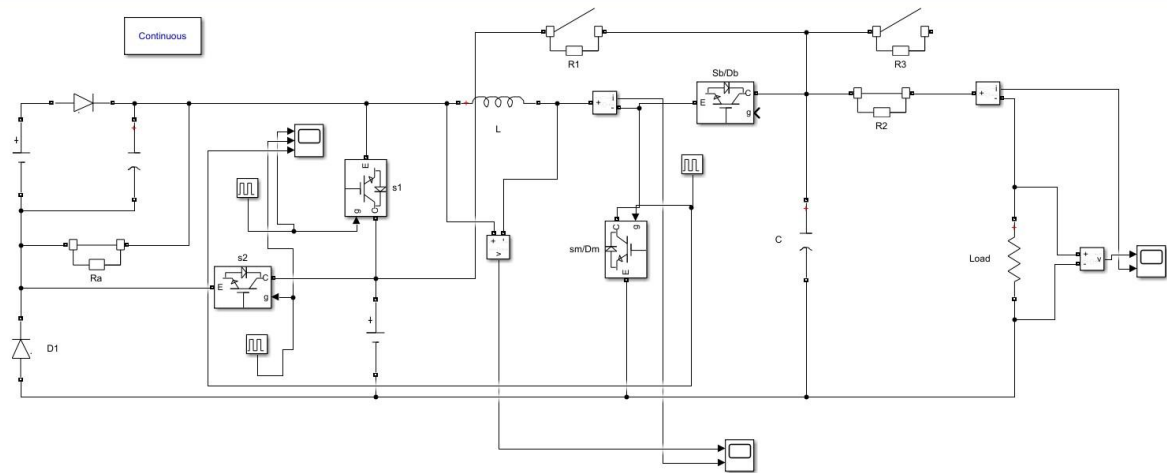


Fig 3.1 Simulation Circuit of C Boost operation

### 3.2 Solar PV-powered operation:

Input source  $V_1$  alone supplies power to the load in type ii operation. The relays  $R_2$  and  $R_A$  are in the active state during this sort of operation, whereas  $R_1$  and  $R_3$  are kept in the off state. Here, there are two operational modes, such as mode 5 and mode 6. While operating in mode 5, the switch  $S_m$  is activated and the inductor stores power from source  $V_1$ . In this mode, the switch  $S_m$  is off, and a voltage of  $V_0 - V_1$  is employed to freewheel the inductor's stored energy into the load. In Fig. 3.3.1 and 3.3.2, the equivalent circuits for each mode are displayed. Assume that  $d_1=d_2=0$  and  $d_3=D$ . The output voltage of the DISOC is controlled by  $S_m$  duty ratio. The output voltage of the DISOC during this operation can be expressed as  $V_0 = \frac{V_1}{1-D}$

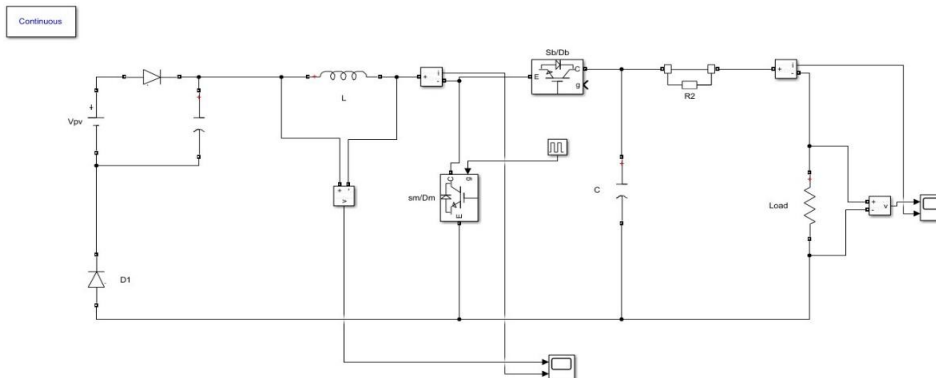
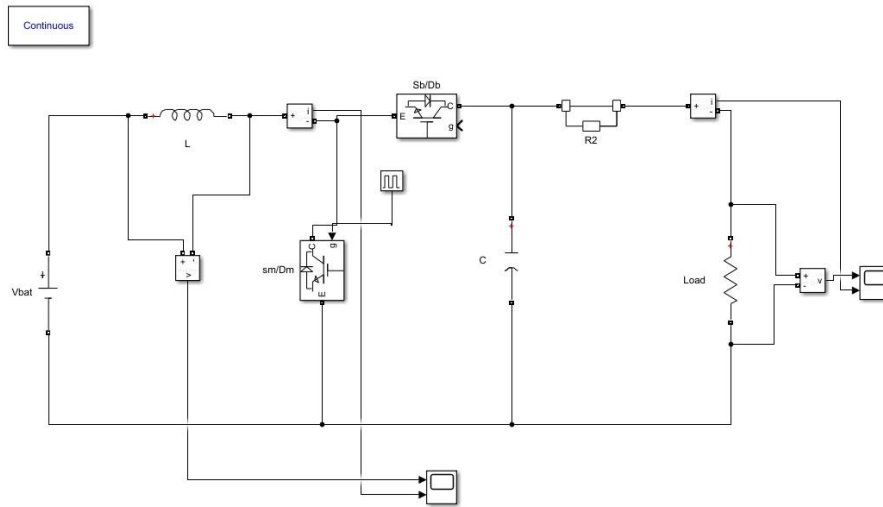


Fig 3.2 Simulation Circuit of PV -powered operation

**3.3 Battery -powered operation:**

The input source  $V_2$  alone power the load in this mode of operation. Two operating modes, shown in fig 3.4.1, are present here as well. According to the analogous circuit depicted as shown in the figure, the remaining relays are kept in the off state while the relay  $R_2$  is kept constantly in the on state. The values of  $d_1=1, d_2=0, d_3=D$ . In this operation, the DISOC's output voltage is stated as  $V_0 = \frac{V_2}{1-D}$



**Fig 3.3 Simulation Circuit of Battery powered operation**

**3.4 Battery charging from solar PV in parking mode:**

To charge the battery using solar PV, the relays  $R_1$  and  $R_A$  are kept turned on, while the rest of the relays are turned off. When solar PV charges the battery, there are two modes of operation. Each mode's equivalent circuits are depicted in Fig4.5 The DISOC output voltage during type when power is delivered from solar PV to the battery is written as  $V_2 = \frac{V_1}{1-D}$

During this operation, the DISOC's output voltage is regulated to the battery charging voltage.

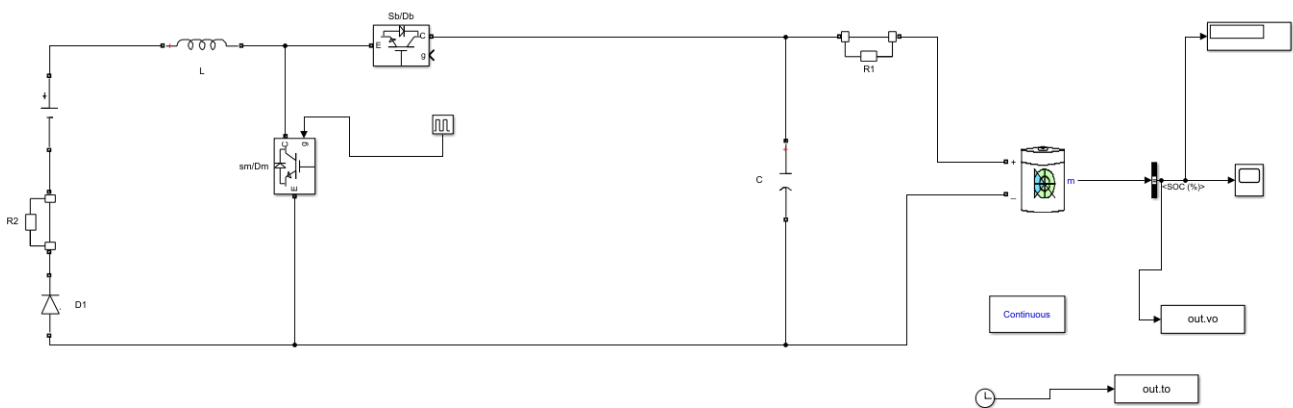


**Fig 3.4 Simulation Circuit of Battery Charging operation**

**3.5 Power flow from V2V or V2G in parking mode:**

To export power from solar PV into the utility grid, the relays  $R_3$  and  $R_A$  are kept turned on, and the rest of the relays are turned off, and are maintained in the off position This Type has two modes of operation. In this case, the type II operation is similar to that of equivalent circuits, except that position of the relay of the switch  $S_m$  duty ratio  $d_3$  governs the output voltage necessary across the DC link of the inverter.

$$V_{Grid} = \frac{V_1}{(1-D)}$$

In practical consideration the output from the converter is given to the inverter circuit and the output of the inverter circuit is given to the Grid or any other

electrical appliances. The output voltage during this mode of operation DC-link voltage of the grid-connected inverter is used to regulate DISOC. When solar energy is used to generate electricity PV to the other EV to enable V2V operation, the DISOC's output voltage is regulated to the battery.

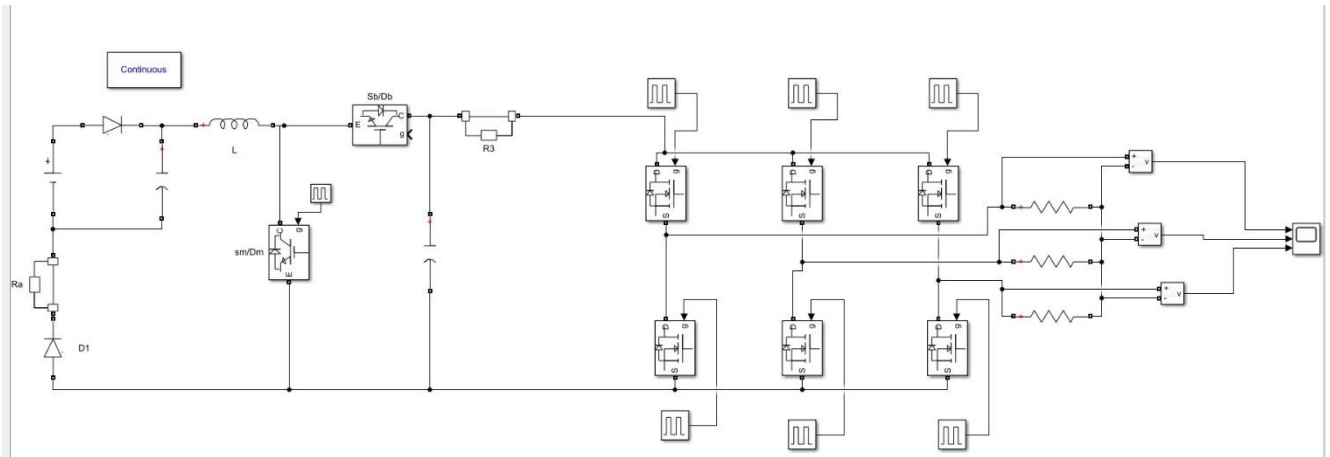


**Fig 3.5 Simulation Circuit of V2V or V2G Operation**

**3.6 Bidirectional rear-buck operation:**

The proposed DISOC has the ability to transfer power bidirectionally between the input sources and the load. This rear-buck mode of operation is used to extract inertial power from the motor during braking. The relays  $R_2$  and  $R_A$  are turned on, while the remaining relays are turned off. The available power in the motor is extracted and returned to the battery. The duty ratio of the switch  $S_{BI}$  controls the power flow from the motor to the battery.

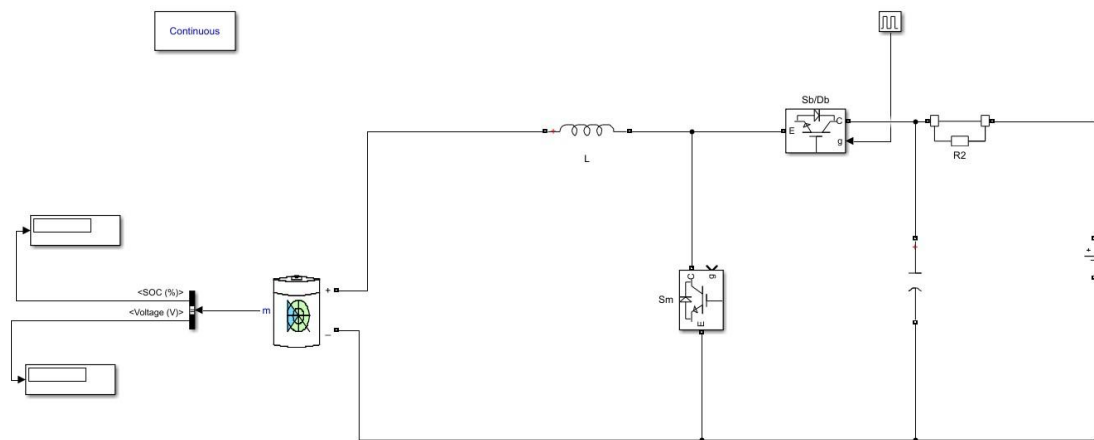
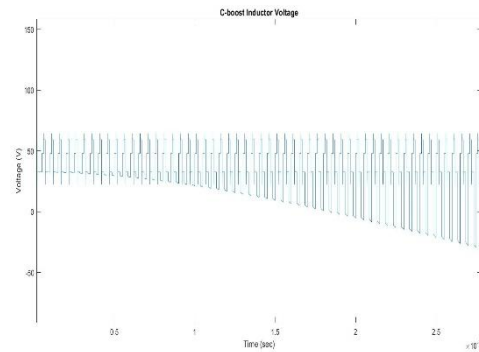
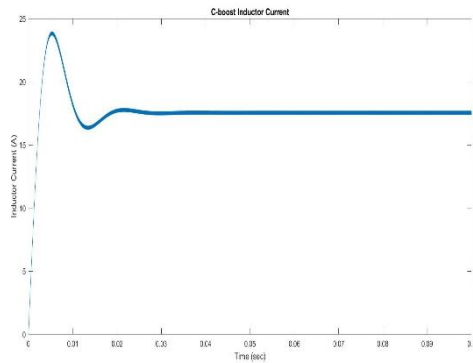
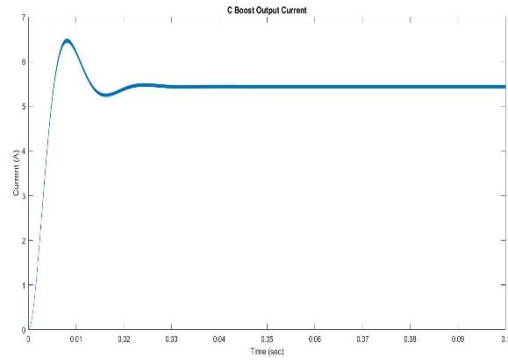
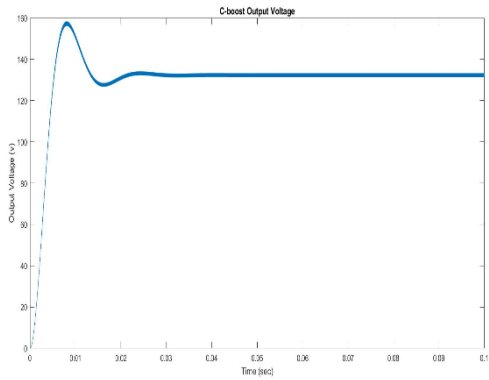


**Fig 3.6 Simulation Circuit of V2V or V2G Operation**

The equivalent circuit diagram of the DISOC in figure 4.7. The switch  $S_{bi}$  is conducting, and the remaining switches are turned off. The inductor stores energy from the load voltage  $V_o$  by passing it through  $S_{BI}$  and  $D_5$ . The figure 3.7.2 Bi-directional converter shows the Bi-directional operation in mode 2. The energy that is stored in the inductor is dissipated to the battery.

The output voltage during the rear buck operation is:  $V_2 = V_o D_{SBI}$

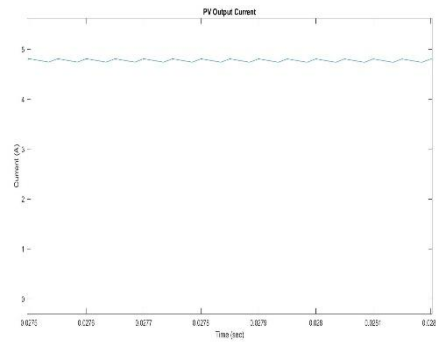
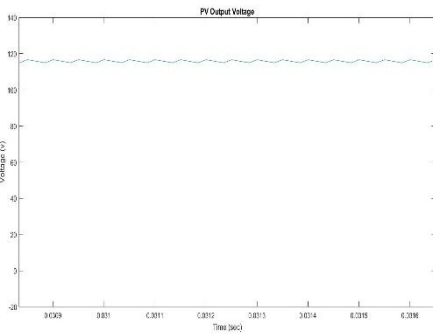
4. Results:



4.1 C-BOOST OPERATION:

Fig 4.1.1 Output Voltage in C-boost Fig 4.1.2 Output current in C-boost

Fig 4.1.3 Inductor current in C-Boost operation Fig 4.1.4 Inductor voltage in C-Boost operation



4.2 Solar PV operation:

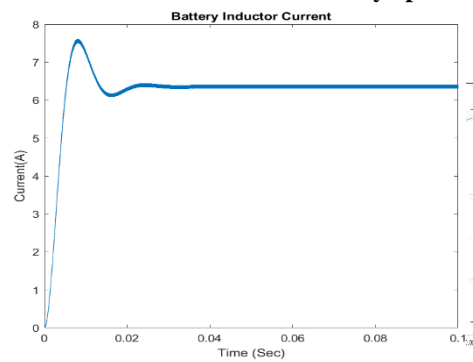
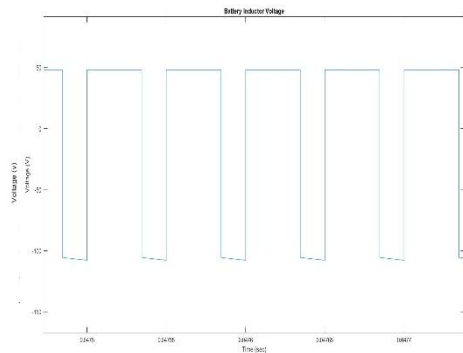
Fig 4.2.1 Output voltage in solar PV

Fig 4.2.2 Output current in solar PV

Fig 4.2.3 Inductor voltage in solar PV

Fig 4.2.4 Inductor current in solar PV

4.3 Battery operation:



**Fig 4.3.1 Inductor voltage in Battery Fig 4.3.2 Inductor Current in Battery  
Fig 4.3.3 output voltage in Battery Fig 4.3.4 output Current in Battery**

**4.4 Battery Charging from PV Cell: 4.5 Power-flow from V2V or V2G in parking mode:**

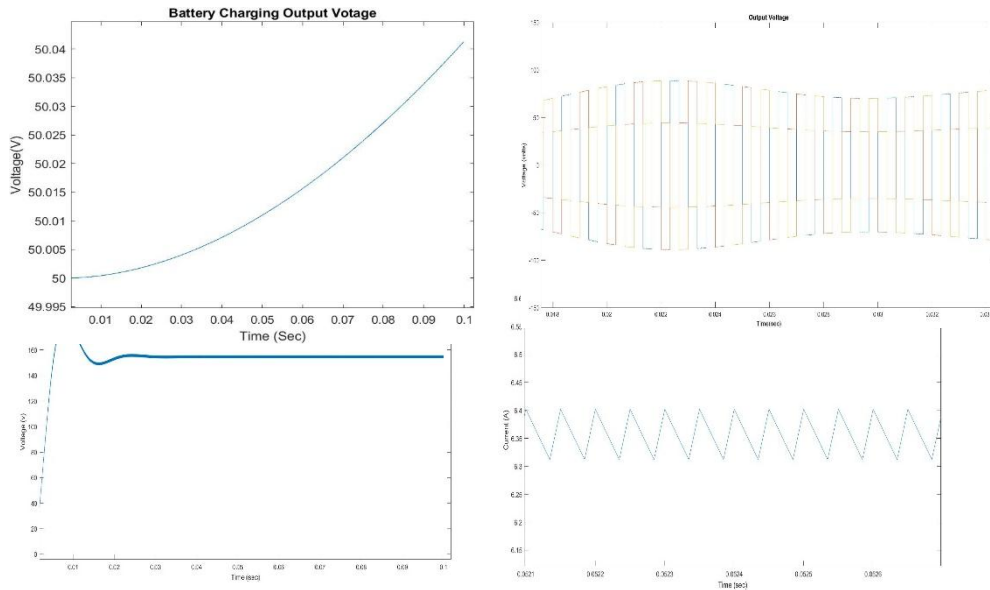


**Fig 4.4.1 output voltage in Battery Charging Fig 4.5.1 output voltage in V2G in Parking operation**

**4.6 Bi - directional rear-buck operation:**

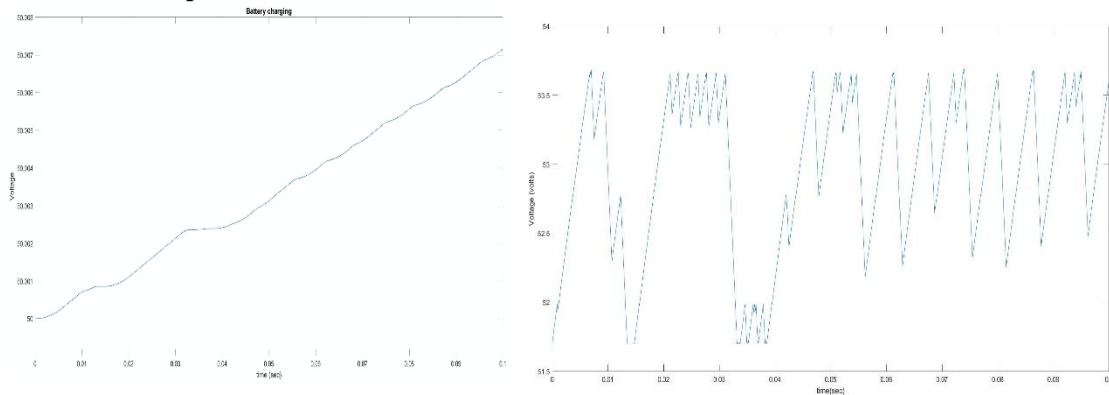


**Fig 4.6.1 output voltage in Battery Charging Fig 4.6.2 output voltage**

**Conclusion:**

Dual Input Single Output converter is presented by integrating with the two different sources. This converter works in six different modes of operation and effectively uses the Solar PV and energy available in the battery. The DISCO converter's advantages make it suitable for solar PV/battery powered electric vehicle applications. Arrangement of relays with the power converter structure is unique and the arrangement of relays help to perform six modes of operation in the proposed DISOC. These modes help for effective utilization of the power present in solar PV and battery. The structure empowers the proposed converter even when any one of the input sources is not available. The switch S2 enables the cascaded operation of the input sources, and achieves a higher output voltage. It has a feature to charge the battery from solar PV by enabling battery charging mode. It utilizes the power available in solar PV and battery to participate in the grid support program by enabling V2G or V2V mode of operation. The key features of the topology are less component count and output voltage.



## REFERENCES

- [1]. A. Nahavandi, M. T. Hagh, M. B. B. Sharifian, and S. Danyali, "A nonisolated multiinput multioutput DC-DC boost converter for electric vehicle applications," *IEEE Trans Power Electron*, vol. 30, no. 4, pp. 1818–1835, Apr. 2015, doi: 10.1109/TPEL.2014.2325830.
- [2]. A. K. Podder, O. Chakraborty, S. Islam, N. Manoj Kumar, and H. H. Alhelou, "Control Strategies of Different Hybrid Energy Storage Systems for Electric Vehicles Applications," *IEEE Access*, vol. 9, pp. 51865–51895, 2021, doi: 10.1109/ACCESS.2021.3069593.
- [3]. M. R. Khalid, I. A. Khan, S. Hameed, M. S. J. Asghar, and J. S. Ro, "A Comprehensive Review on Structural Topologies, Power Levels, Energy Storage Systems, and Standards for Electric Vehicle Charging Stations and Their Impacts on Grid," *IEEE Access*, vol. 9. Institute of Electrical and Electronics Engineers Inc., pp. 128069–128094, 2021. doi: 10.1109/ACCESS.2021.3112189.
- [4]. A. Khaligh and Z. Li, "Battery, ultracapacitor, fuel cell, and hybrid energy storage systems for electric, hybrid electric, fuel cell, and plug-in hybrid electric vehicles: State of the art," *IEEE Trans Veh Technol*, vol. 59, no. 6, pp. 2806–2814, Jul. 2010, doi: 10.1109/TVT.2010.2047877.
- [5]. C. Zheng, W. Li, and Q. Liang, "An Energy Management Strategy of Hybrid Energy Storage Systems for Electric Vehicle Applications," *IEEE Trans Sustain Energy*, vol. 9, no. 4, pp. 1880–1888, Oct. 2018, doi: 10.1109/TSTE.2018.2818259.
- [6]. H. S. Salama, S. M. Said, M. Aly, I. Vokony, and B. Hartmann, "Studying Impacts of Electric Vehicle Functionalities in Wind Energy-Powered Utility Grids with Energy Storage Device," *IEEE Access*, vol. 9, pp. 45754–45769, 2021, doi: 10.1109/ACCESS.2021.3066877.
- [7]. Y. Bai, J. Li, H. He, R. C. dos Santos, and Q. Yang, "Optimal Design of a Hybrid Energy Storage System in a Plug-In Hybrid Electric Vehicle for Battery Lifetime Improvement," *IEEE Access*, vol. 8, pp. 142148–142158, 2020, doi: 10.1109/ACCESS.2020.3013596.
- [8]. L. Zhang, X. Hu, Z. Wang, F. Sun, J. Deng, and D. G. Dorrell, "Multiobjective Optimal Sizing of Hybrid Energy Storage System for Electric Vehicles," *IEEE Transactions on Vehicular Technology*, vol. 67, no. 2. Institute of Electrical and Electronics Engineers Inc., pp. 1027–1035, Feb. 01, 2018. doi: 10.1109/TVT.2017.2762368.
- [9]. J. Shen and A. Khaligh, "A supervisory energy management control strategy in a battery/ultracapacitor hybrid energy storage system," *IEEE Transactions on Transportation Electrification*, vol. 1, no. 3, pp. 223–231, Oct. 2015, doi: 10.1109/TTE.2015.2464690.
- [10]. V. K. Goyal and A. Shukla, "Isolated DC-DC Boost Converter for Wide Input Voltage Range and Wide Load Range Applications," *IEEE Transactions on Industrial Electronics*, vol. 68, no. 10, pp. 9527–9539, Oct. 2021, doi: 10.1109/TIE.2020.3029479.
- [11]. H. L. Jou, J. J. Huang, J. C. Wu, and K. der Wu, "Novel isolated multilevel DC-DC power converter," *IEEE Trans Power Electron*, vol. 31, no. 4, pp. 2690–2694, Apr. 2016, doi: 10.1109/TPEL.2015.2487558.
- [12]. J. M. Kwon, E. H. Kim, B. H. Kwon, and K. H. Nam, "High-efficiency fuel cell power conditioning system with input current ripple reduction," in *IEEE Transactions on Industrial Electronics*, 2009, vol. 56, no. 3, pp. 826–834. doi: 10.1109/TIE.2008.2004393.
- [13]. G. G. Kumar and K. Sundaramoorthy, "Dual-Input Nonisolated DC-DC Converter With Vehicle-to-Grid Feature," *IEEE J Emerg Sel Top Power Electron*, vol. 10, no. 3, pp. 3324–3336, Jun. 2022, doi: 10.1109/JESTPE.2020.3042967.
- [14]. Manoj, V., Sravani, V., Swathi, A. 2020. A multi criteria decision making approach for the selection of optimum location for wind power project in India. EAI Endorsed Transactions on Energy Web, 8(32), e4
- [15]. J. T. Bialasiewicz, "Renewable energy systems with photovoltaic power generators: Operation and modeling," *IEEE Trans. Ind. Electron.*, vol. 55, no. 7, pp. 2752–2758, Jul. 2008
- [16]. MNRE (Ministry of New and Renewable Energy), Grid Connected Power/Solar. 2018.
- [17]. S. Kouro, J. I. Leon, D. Vinnikov, and L. G. Franquelo, "Grid-connected photovoltaic systems: An overview of recent research and emerging PV converter technology," *IEEE Ind. Electron. Mag.*, vol. 9, no. 1, pp. 47–61, Mar. 2015.
- [18]. Dinesh, L., Sesham, H., & Manoj, V. (2012, December). Simulation of D-Statcom with hysteresis current controller for harmonic reduction. In 2012 International Conference on Emerging Trends in Electrical Engineering and Energy Management (ICETEEEM) (pp. 104-108). IEEE
- [19]. Manoj, V. (2016). Sensorless Control of Induction Motor Based on Model Reference Adaptive System (MRAS). International Journal For Research In Electronics & Electrical Engineering, 2(5), 01-06.
- [20]. V. B. Venkateswaran and V. Manoj, "State estimation of power system containing FACTS Controller and PMU," 2015 IEEE 9th International Conference on Intelligent Systems and Control (ISCO), 2015, pp. 1-6, doi: 10.1109/ISCO.2015.7282281
- [21]. Manohar, K., Durga, B., Manoj, V., & Chaitanya, D. K. (2011). Design Of Fuzzy Logic Controller In DC Link To Reduce Switching Losses In VSC Using MATLAB-SIMULINK. Journal Of Research in Recent Trends.
- [22]. Manoj, V., Manohar, K., & Prasad, B. D. (2012). Reduction of switching losses in VSC using DC link fuzzy logic controller Innovative Systems Design and Engineering ISSN, 2222-1727
- [23]. Dinesh, L., Harish, S., & Manoj, V. (2015). Simulation of UPQC-IG with adaptive neuro fuzzy controller (ANFIS) for power quality improvement. Int J ElectrEng, 10, 249-268
- [24]. Manoj, V., Swathi, A., & Rao, V. T. (2021). A PROMETHEE based multi criteria decision making analysis for selection of optimum site location for wind energy project. In IOP Conference Series: Materials Science and Engineering (Vol. 1033, No. 1, p. 012035). IOP Publishing.
- [25]. Kiran, V. R., Manoj, V., & Kumar, P. P. (2013). Genetic Algorithm approach to find excitation capacitances for 3-phase smseig operating single phase loads. Caribbean Journal of Sciences and Technology (CJST), 1(1), 105-115.
- [26]. Manoj, V., Manohar, K., & Prasad, B. D. (2012). Reduction of Switching Losses in VSC Using DC Link Fuzzy Logic Controller. Innovative Systems Design and Engineering ISSN, 2222-1727.
- [27]. Manoj, V., Krishna, K. S. M., & Kiran, M. S. Photovoltaic system based grid interfacing inverter functioning as a conventional inverter and active power filter.